

Experimental and Numerical Studies of Heat Transfer Characteristics for Impinging Jet on Dimple Surfaces

Parkpoom Sriromreun^{a,c,*}, Paranee Sriromreun^{b,c}

^aDepartment of Mechanical Engineering, Faculty of Engineering, Srinakharinwirot University, Ongkharak, Nakhorn-Nayok, 26120, Thailand

^bDepartment of Chemical Engineering, Faculty of Engineering, Srinakharinwirot University, Ongkharak, Nakhorn-Nayok, 26120, Thailand

^cThe Graduate school of Srinakharinwirot University, Srinakharinwirot University 114 Sukhumvit 23, Bangkok 10110, Thailand
 prakpum@g.swu.ac.th

Experimental and numerical works have been carried out to investigate the effect of impingement dimples surface on heat transfer characteristics in a circular test plate. Impingement jet technique and dimple shape can enhance the heat transfer rate caused by the high turbulence intensity. The cylindrical shape of dimple was used in this work. The simulation results were validated with the experimental data obtained from 4 types test plates. The simulate data displayed the flow structure and contour temperature surface on the test plate which provided the complex flow and heat transfer characteristics. The experimental results showed that the case of the dimple diameter (d) equal to the jet diameter (D_j), and the distance between jet and the test plate (B) is 2 times of D_j , yielded the maximum heat transfer rate. The heat transfer rate enhanced up to 200 % compared to a flat plate at $Re_j = 14,500$.

1. Introduction

For decades, the development of heat exchanger systems has been made to improve the heat transfer rate and cost savings. A high-performance heat exchanger is needed in many engineering applications such as chemical engineering, refrigeration, automobile manufacturing and solar air heater for using an energy source efficiently leading to the reduction of size and cost of the heat exchanger, and energy saving. A jet impingement onto a surface is one way of high effective for promoting high rates of heat transfer (Nanan et al., 2012) because the impingement creates the fluid flow contacting the surface very well. Therefore, the impingement can be used to solve the problem of fluid flow in the core, which does not connect to the surface of heat exchanger (Pakhomov, 2010). In addition, baffles/ribs/fins/dimples have been applied extensively in order to alter flow pattern of the heat exchangers. The using of baffles/ribs/fins leads to high friction loss because of the obstruction of fluid flow while the dimples give low friction loss due to the absence of the obstruction of fluid flow. In general, the dimples are employed to generate vortex flows that can induce high flow mixing between the core and the near-wall regions resulting an increasing in heat transfer rate and low-pressure loss (Turnow et al., 2012). The surface of dimples can be modified in many applications for heat exchanger (Gradeck et al., 2011). Several investigations on the effect of those parameters of impinging air jet on the heat transfer for many roughened surface geometries have been conducted widely. Bonis et al. (2011) applied the impingement technique for food drying or dehydration. The heat transfer rate, water activity and moisture depletion had been measured in a food substrate using a turbulent air jet impingement for food heating. Parida et al. (2011) studied the jet impingement for cooling high heat flux (i.e. cutting-edge electronic technologies). The results show that developments in cooling methodologies were therefore required to avoid unacceptable temperature rise, and also to maintain a high performance. An overall improvement in quality of 150 % - 200 % in the maximum Nu recorded both experimentally and numerically was effect from impingement and associated swirl.

The literature survey cited above presents the use of semi-sphere shape of dimple. In this work, the cylinder shape of dimple will be introduced because of its simply manufacturing (Govindaraj et al., 2017). The testing fluid was air and was presented in impinging jet flows for $Re_j = 1,450$ to 14,500. The distance confinement plate

height over the test plate (B) was varied 2, 4 and 6 times of jet diameter (D_j). The dimple diameter is 1, and 2 times of D_j . The numerical investigation of the flow structure and temperature contour of impact jet on test plate also investigated.

2. Experimental setup

The test section is shown in Figure 1a by using air as the test fluid. The details of the impingement dimples surface are shown in Figure 1b. In Figure 1a, the air compressor with the tank were used to blow the air through the long pipe with 20 mm internal diameter and through the jet with 10 mm diameter (D_j), then percolate to the impingement plate. The impingement dimple surface was made of copper circular plate. In order to measure temperature distributions on the impingement plate, 16 thermocouples were fitted into the test plate. The thermocouples were installed in holes drilled from the rear face with the respective junctions positioned within 1.5 mm of the inside wall. 2 RTD-type thermocouples for inlet and outlet test section were calibrated within ± 0.2 °C deviation by thermostat before being used. The thermocouple voltage outputs were fed into the data acquisition system and then recorded via a computer.

The heater was installed on the bottom wall of the test section to maintain uniform surface heat flux. The electrical output power was controlled by a variac transformer to obtain a constant heat flux. In Figure 1, the diameter of the plate (D) is 300 mm. The diameters of cylindrical dimples are 10 and 20 mm (d) with the distance between dimples in radial, $E_r = 2d$, and the dimple distances along the circumference, $E_\theta = 1.5d$. The confinement plates are 20, 40 and 60 mm (B) is above the test plate.

The uncertainty in the data calculation was based on ANSI/ASME (1986). The uncertainty in the velocity measurement was estimated to be less than ± 7 %, whereas that of wall temperature measurement was about ± 0.5 %. The maximum uncertainties of non-dimensional parameters were ± 5 % for Nusselt number, and ± 5 % for Reynolds number.

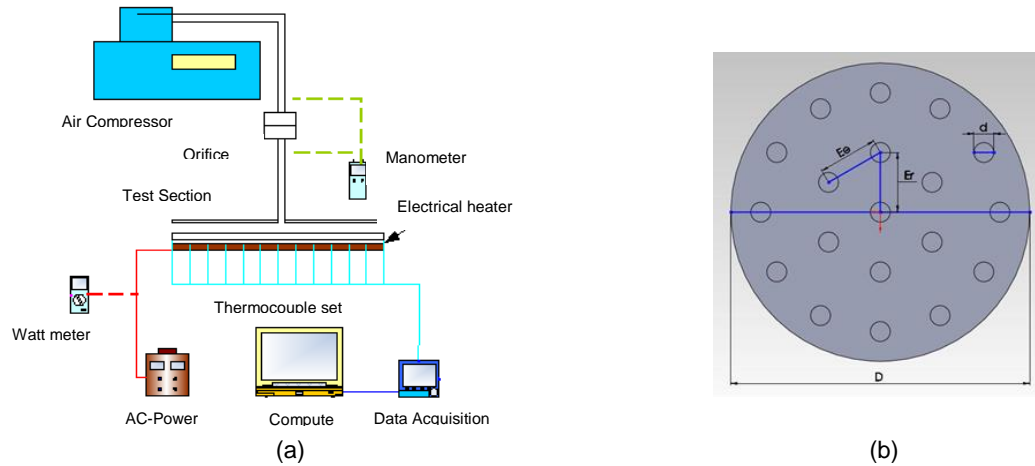


Figure 1: (a) Schematic diagram of experimental apparatus and (b) details of the impingement dimples surface.

3. Data reduction

Inlet-outlet temperature (T_{in} and T_{out}) of test section were obtained from the experiment, which were used to calculate in another form because they can be described heat transfer characteristics. The local heat transfer coefficient (h) and average heat transfer coefficient (\bar{h}) (Incropera, 1996) were determined from the temperatures as shown in Eq(1) and Eq(2).

$$Q = mC_p(T_{in} - T_{out}) = hA_s(T_s - T_b) \quad , \quad h = mC_p(T_{out} - T_{in})/A_s(T_s - T_b) \quad (1)$$

$$\bar{h} = \frac{2\pi \int_0^{R/R_o} h \left(\frac{r}{R_o} \right) d \left(\frac{r}{R_o} \right)}{\pi \left(\frac{R^2}{R_o} \right)} \quad , \quad T_b = (T_{out} + T_{in})/2 \quad (2)$$

In which r/R_o is a dimensionless radius measured from the jet centerline and R/R_o is the dimensionless radius as defined in Eq(2). The value of \bar{h} at a given radial location (R) is the effective heat transfer coefficient for the entire disk from $r = 0$ to $r = R$. The term, \bar{h} is the inner surface area of the heated walls, whereas T_s is the local surface temperature on the impingement plate of the heated surface. The term m and C_p are mass flow rate and specific heat at constant pressure, respectively. Then, local Nusselt number (Nu) and average Nusselt number (\bar{Nu}) were calculated from the local and average heat transfer coefficients, respectively as shown in Eq(3). It represents the performance of the heat transfer.

$$Nu = \frac{hD_{hj}}{K}, \quad \bar{Nu} = \frac{\bar{h}D_{hj}}{K} \quad (3)$$

4. Simulation of flow configuration

In this research flow pattern and temperature distribution on a test plate were simulated using a CFD program. The CFD technique reduces the number of necessary experiments and gives results, which would hardly be accessible by measurements (Patankar, 1980). The flow system is a vertical cylindrical channel with dimple repeatedly placed on imping wall (lower wall for ease of observation in the present case) as depicted in Figure 2a. The detail of the channel is shown in Figure 2a, whereas a module of the computational domain due to symmetry flow along the radius is displayed in Figure 2b.

For the channel model, a uniform air velocity at 300K ($P_r = 0.707$) is introduced at the inlet while a pressure outlet condition is applied at the exit. The physical properties of the air have been assumed to remain constant at the initial air temperature. Impermeable boundary and no-slip wall conditions have been implemented over the channel walls as well as the dimple surface apart from the enhanced wall treatment. The lower wall is heated with a constant heat flux while the dimple surface is assumed at adiabatic wall (high thermal resistance) conditions. The geometry of computational domain dimensions was the same to the dimensions of the experimental setup section. The geometry and the mesh preparation for the geometry was performed with gambit version 2.2.30. The smooth channel was employed in the current investigation.

The numerical model for fluid flow and heat transfer in the channel is developed under the following assumptions: steady, three-dimensional, turbulent, incompressible flow, constant fluid properties, ignored body forces, viscous dissipation and radiation heat transfer (Sarghini et al., 2017). Based on the above assumptions, the channel flow model is governed by the Reynolds averaged Navier–Stokes (RANS) equations with the $k-\epsilon$ turbulence model and the energy equation. The $k-\epsilon$ and RNG model in ANSYS program were used to simulate the turbulent flow. The details on mathematical modeling can be found in Promvong et al. (2011).

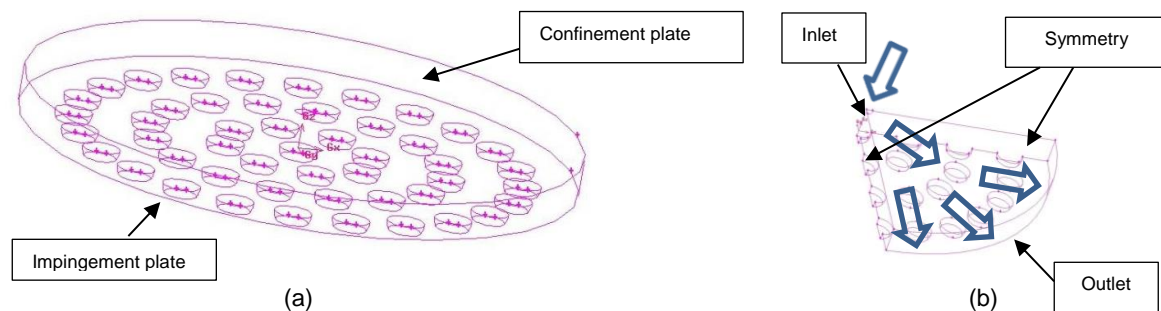


Figure 2: (a) Channel geometry and (b) Computational domain of flow.

5. Results and discussion

5.1 Effect of dimples shape

The experimental results are reported comparing between flat plate and dimple surface in Figure 3, which display the comparison of heat transfer rate in term of Nusselt number. In Figure 3, the average Nusselt number (\bar{Nu}) tends to increase with increasing the Reynolds number. The results showed that the plate with dimple provides higher heat transfer rate than that of the flat plate for all Reynolds numbers ($Re = 1,450$ to $14,500$). These Reynolds numbers were calculated at the jet pipe. However, flow characteristics in test plate were turbulence flow for all Re . The dimple surfaces led to stronger impingement flow and higher heat transfer rate.

The mean Nusselt number increased from using the dimple plate was found to be about 200 % over the flat plate.

5.2 Effect of the distance between test plate and jet (B)

From Figure 3, the average Nusselt number increased with decreasing the distance between test plate and jet (B). The dimple size (d) that is equal to the jet diameter (D_j) and $B = 2D_j$, $4D_j$ and $6D_j$ at $Re = 14,500$ indicates about 100, 75 and 45, respectively.

5.3 Effect of dimple diameter (d)

The effects of the dimple diameter (d) with two value $d = D_j$, $2D_j$ for test plate on heat transfer rate in \overline{Nu} is depicted in Figure 3. For the test plate at $d = D_j$ is much higher than that of the test plate at $d = 2D_j$. The test plate with $B = 2D_j$ at $d = D_j$ showed the highest heat transfer rate than the test plate at $d = 2D_j$ around 170 %, because of a higher number of diameter provided more vortex flow and higher turbulence intensity.

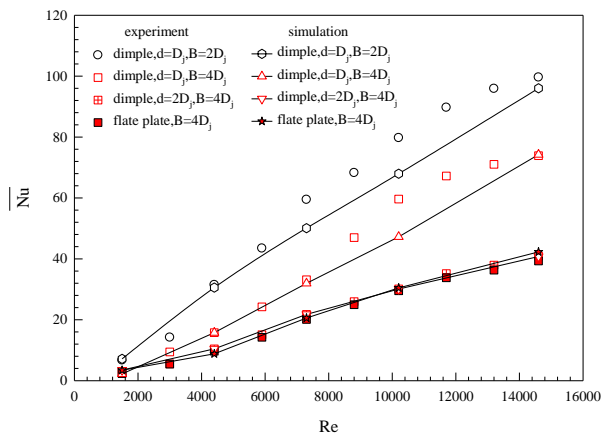


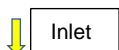
Figure 3: Variation of \overline{Nu} with Re for flat plate and dimple plate is $E_r=2d$ and $E_r=1.5d$.

5.4 Simulation of impinging jet on dimple surface

The comparison between the experimental and simulation works are shown in Figure 3. It is worth noting that the numerical results are in good agreement with measurements. The discrepancies for the \overline{Nu} values are less than $\pm 10\%$ (Sriromreun et al., 2017).

The streamlines in Figure 4 show the air flow directions over the test plate with $B = 4D_j$ at the same $Re = 14,600$ for 3 cases: (a) Flat plat, (b) $d = D_j$ and (c) $d = 2D_j$. Figure 4 displays the velocity vector along the radial direction of the test plate. In Figure 4a, the impinging flow can help to increase the heat transfer rate from fluid flow to impact heat flat plate directly, which effects on the increasing of the temperature different between the heated wall and the cold fluid. Figure 4b, and 4c show that the dimple can induce co-vortex flows along the test channel, leading to high turbulence intensity. The streamline demonstrated that co-rotating vortices or longitudinal vortex flows caused by the dimple. The longitudinal vortex flows enhanced heat transfer rate in the test plate.

Figure 5 shows streamlines on the dimple plate with $d = D_j$ and $B = 2D_j$ in 5 cases: (a) $Re = 1,500$, (b) 4,400, (c) 10,200 and (d) 14,600. Higher Re displays higher velocity and higher turbulence intensity. This effects enhanced heat transfer coefficient. Figure 6 represents the temperature surface contours in quarter of test plate for using the dimple in 3 cases: (a) Dimple: $d = D_j$, $B = 2D_j$, (b) Dimple: $d = D_j$, $B = 4D_j$, (c) Dimple, $d = 2D_j$, $B = 4D_j$ at $Re = 14,600$. Temperature surface contours were about 620°C around centre of the plate and the temperatures are increased while the radius are increased. Case (b) shows the highest obtained temperature which is about 660°C . Temperature on the surface presented the performance of heat transfer from test plate. Low temperature indicated good heat transfer, while high temperature refers to bad heat transfer. Case (b) was not good performance of heat transfer rate, because the position of the air jet inlet was far from test plate ($B = 4D_j$).



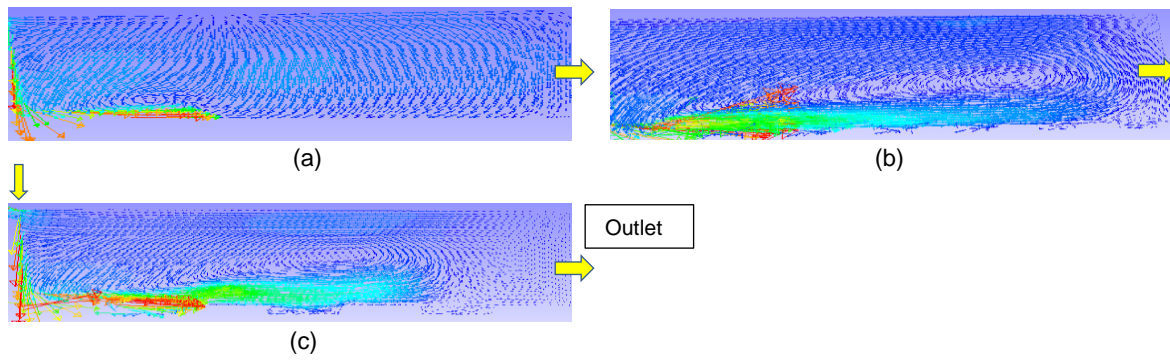


Figure 4: Streamlines with $B = 4D_j$ at $Re = 14,600$ (a) Flat plate, (b) $d = D_j$ and (c) $d = 2D_j$.

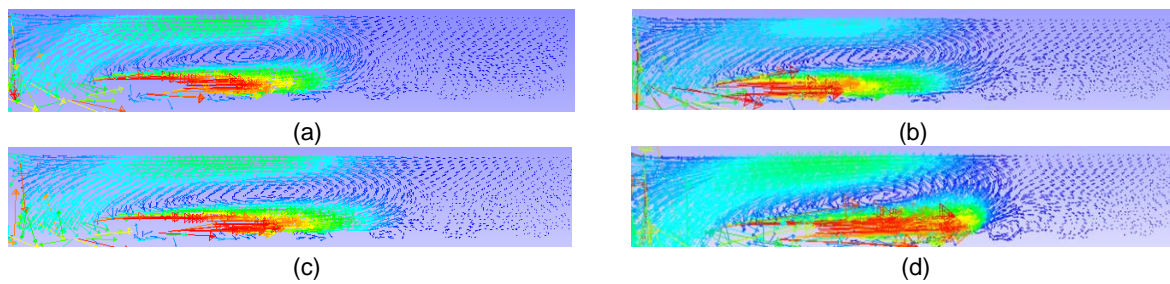


Figure 5: Streamlines with $d = D_j$ and $B = 2D_j$ at (a) $Re = 1,500$, (b) $Re = 4,400$, (c) $Re = 10,200$ and (d) $Re = 14,600$.

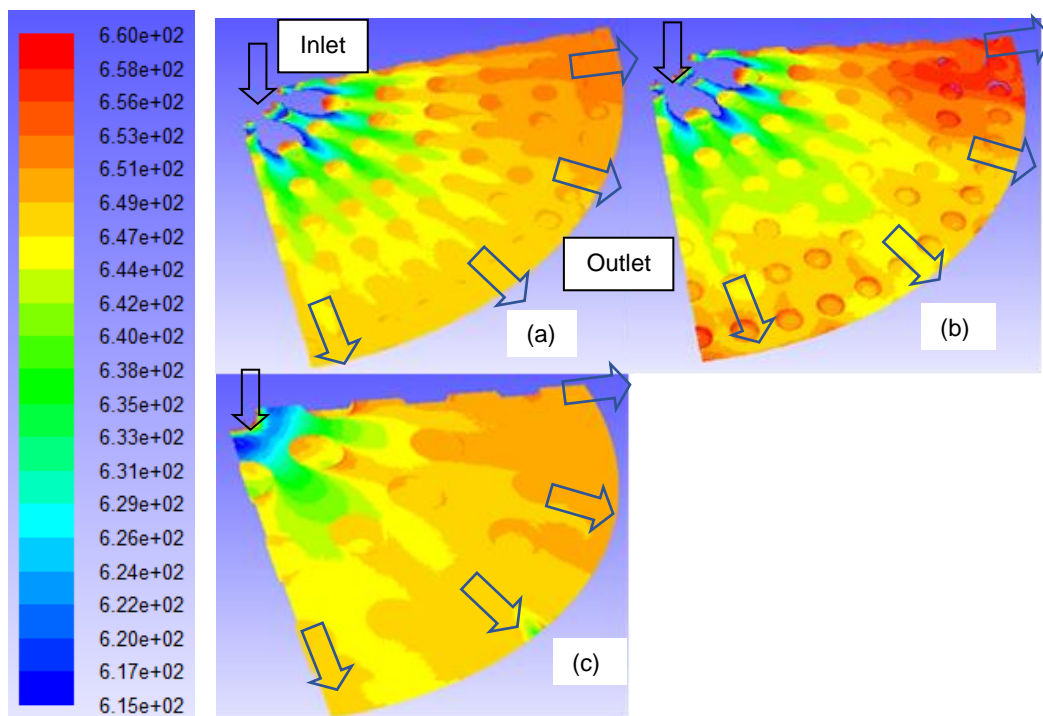


Figure 6: Temperature contours at $Re = 14,600$ (a) $d = D_j$, $B = 2D_j$; (b) $d = D_j$, $B = 4D_j$ and (c) $d = 2D_j$, $B = 4D_j$.

6. Conclusions

An experimental and numerical studies were conducted to examine the heat transfer characteristics in a circle test plate diameter (D), which is 30 times of diameter jet (D_j) in the turbulent regime from $Re = 1,450$ to $14,500$. The Nu values depend on the dimple diameter (d), the distance between test plates and jet (B), and Reynolds number. While a decrease in d and B lead to increase the Re and the \overline{Nu} . The dimple plates indicates the better heat transfer than the flat plat. The dimple plate with $d = D_j$, $B = 2D_j$, $E_r = 2d$ and $E_\theta = 1.5d$ provided the highest at about 100 at the $Re = 14,500$. Simulation results displayed the flow structure of impingement jet and the temperature contour on the test plate. The result showed the contrast of flat plate and dimple plates. The dimple plate is stronger turbulence intensity than the flat plate. The narrow B and the small d of dimple plate indicate higher heat transfer rate and turbulence intensity. This research can be applied in impinging jet on surface of heat exchanger i.e. blowing cool air to decrease temperature of hot food product.

Acknowledgments

The funding of this research work is supported by the Research Grants of Faculty of Engineering 2016, Srinakharinwirot University (SWU, Grant number: 579/2016). The authors also greatly acknowledged the Graduate school of Srinakharinwirot University for conference presentation grant.

References

- ANSI/ASME, 1986, Measurement uncertainty Part I., PTC, ASME Standards, New York, USA.
- Bonis M.V.De., Ruocco G., 2011, An experimental study of the local evolution of moist substrates under jet impingement drying, *International Journal of Thermal Sciences*, 50(1), 81-87.
- Govindaraj K., Panchabikesan K., Denkenberger D.C., Ramalingam V., 2017, Effect of fin orientations in a spherically encapsulated phase change materials for effective heat transfer enhancement, *Chemical Engineering Transactions*, 62, 277-282.
- Gradeck M., Ouattara A., Maillet D., Gardin P., Lebouché M., 2011, Heat transfer associated to a hot surface quenched by a jet of oil-in-water emulsion, *Experimental Thermal and Fluid Science*, 35, 841-847.
- Incropera F., Dewitt P.D., 1996, Introduction to Heat Transfer, third ed., John Wiley & Sons Inc, New York.
- Nanan K., Wongcharee K., Nuntadusit C., Eiamsa-ard S., 2012, Forced convective heat transfer by swirling impinging jets issuing from nozzles equipped with twisted tapes, *International Communications in Heat and Mass Transfer*, 39, 844-852.
- Pakhomov M.A., Terekhov V.I., 2010, Enhancement of an impingement heat transfer between turbulent mist jet and flat surface, *International Journal of Thermal Sciences*, 53, 3156–3165.
- Parida P.R., Ekkad S.V., Ngo K., 2011, Experimental and numerical investigation of confined oblique impingement configurations for high heat flux applications, *International Journal of Thermal Sciences* 50(1), 1037-1050.
- Patankar S.V., 1980, Numerical heat transfer and fluid flow, Hemisphere Publishing Corporation, Taylor and Francis Group, New York, USA.
- Promvong P., Changcharoen W., Kwankaomeng S., Thianpong C., 2011, Numerical heat transfer study of turbulent square-duct flow through inline V-shaped discrete ribs, *International Communications of Heat and Mass Transfer*, 38(10), 1392-1399.
- Sarghini F., Vivo A.De., Erdogdu F., 2017, Analysis of Heat and Momentum Transfer in Screw-Drive Heat Transfer Systems, *Chemical Engineering Transactions*, 57, 1729-1734.
- Sriromreun P., Sriromreun P., 2017, Numerical study on heat transfer enhancement in a rectangular duct with incline shaped baffles, *Chemical Engineering Transactions*, 57, 1243-1248.
- Turnow J., Kornev N., Zhdanov V., Hassel E., 2012, Flow structures and heat transfer on dimples in a staggered arrangement, *International Journal of Heat and Fluid Flow*, 35, 168–175.